ЖЭТФ, 2022, том 162, вып. 4 (10), стр. 455–462

CONDUCTIVITY OF TWO-DIMENSIONAL SMALL GAP SEMICONDUCTORS AND TOPOLOGICAL INSULATORS IN STRONG COULOMB DISORDER

Yi Huang (黄奕) [a*], ***B. I. Shklovskii*** [a], ***Brian Skinner*** [b]

[a] *School of Physics and Astronomy, University of Minnesota Minneapolis, Minnesota 55455, USA*

[b] *Department of Physics, The Ohio State University, Columbus Ohio 43202, USA*

Received May 29, 2022,
revised version May 29, 2022
Accepted June 1, 2022

We are honored to dedicate this article to Emmanuel Rashba on the occasion of his 95 birthday. In the ideal disorder-free situation, a two-dimensional band gap insulator has an activation energy for conductivity equal to half the band gap, Δ. But transport experiments usually exhibit a much smaller activation energy at low temperature, and the relation between this activation energy and Δ is unclear. Here we consider the temperature-dependent conductivity of a two-dimensional narrow gap semiconductor on a substrate containing Coulomb impurities, mostly focusing on the case when amplitude of the random potential $\Gamma \gg \Delta$. We show that the conductivity generically exhibits three regimes and only the highest temperature regime exhibits an activation energy that reflects the band gap. At lower temperatures, the conduction proceeds through nearest-neighbor or variable-range hopping between electron and hole puddles created by the disorder. We show that the activation energy and characteristic temperature associated with these processes steeply collapse near a critical impurity concentration. Larger concentrations lead to an exponentially small activation energy and exponentially long localization length, which in mesoscopic samples can appear as a disorder-induced insulator-to-metal transition. We arrive at a similar disorder driven steep insulator–metal transition in thin films of three-dimensional topological insulators with very large dielectric constant, where due to confinement of electric field internal Coulomb impurities create larger disorder potential. Away from neutrality point this unconventional insulator-to-metal transition is augmented by conventional metal–insulator transition at small impurity concentrations, so that we arrive at disorder-driven re-entrant metal–insulator–metal transition. We also apply this theory to three-dimensional narrow gap Dirac materials.

Contribution for the JETP special issue in honor of E. I. Rashba's 95th birthday

DOI: 10.31857/S0044451022100029
EDN: EMVOJE

1. INTRODUCTION

In a band gap insulator, charged impurities often play a decisive role in determining the properties of the insulating state. Due to the long-ranged nature of the Coulomb potential that they create, such impurities produce large band bending that changes qualitatively the nature of electron conduction relative to the ideal disorder-free situation. An illustrative case is that of a three-dimensional completely-compensated semiconductor, for which positively-charged donors and negatively-charged acceptors are equally abundant and randomly distributed in space. In this case, the impurity potential has large random fluctuations, which can be screened only when the amplitude of this potential reaches Δ, where 2Δ is the band gap. This screening is produced by sparse electron and hole droplets, concentrated in spatially alternating electron and hole clouds (puddles) [1–3] (see Fig. 1). At high enough temperatures the electrical conductivity is due to activation of electrons and holes from the Fermi level to the energy

* E-mail: huan1756@umn.edu

associated with classical percolation across the sample. At lower temperatures the conductivity is due to hopping between nearest neighbor puddles (NNH). At even smaller temperatures it is due to variable range hopping (VRH) between puddles. Crucially, in each of these temperature regimes the naive relation $E_a = \Delta$ is lost, where E_a is the activation energy for conductivity. Only in the highest temperature regime is there a direct proportionality between E_a and Δ (with a non-trivial small numeric prefactor) [3, 4]; at lower temperatures the observed activation energy is non-universal and disorder-dependent [1, 2].

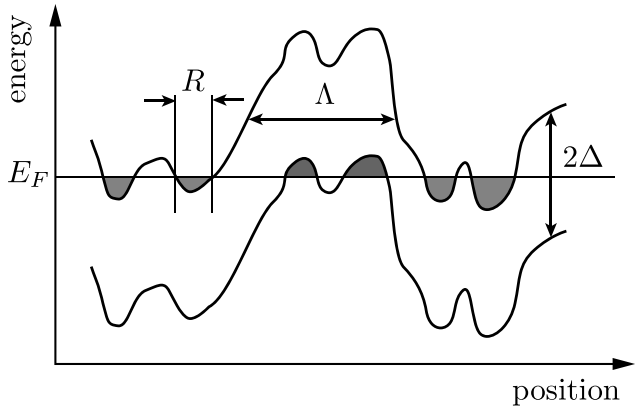

Fig. 1. Schematic energy diagram of a completely compensated semiconductor with relatively weak disorder. The wavy lines show the conduction band bottom and the valence band ceiling separated by the gap 2Δ. Droplets of holes are shaded by red, while electron droplets are shaded by blue. Here R is the size of a droplet, and Λ is the size of a droplet cloud (puddle), which contains several droplets

In this paper we consider a similar problem in two dimensions. Specifically, we consider a two-dimensional small band gap semiconductor resting on a thick substrate with a three-dimensional concentration of randomly-positioned impurities and focus on the case when $\Gamma \gg \Delta$ (see Fig. 2). We derive the temperature dependence of the electrical conductivity across all temperature regimes and show that the observed activation energy of the conductivity can be very small.

Understanding the relation between the energy gap and the observed activation energy for transport is of crucial importance for studying a variety of new 2D electron systems. For example, recent studies of 2D topological insulators (TIs) [5–7], films of 3D TIs [8–24], bilayer graphene (BLG) with an orthogonal electric field [25, 26] and twisted bilayer graphene (TBG) [27–31] use the transport activation energy as a way of characterizing small energy gaps. In all these cases the observed activation energy is much smaller

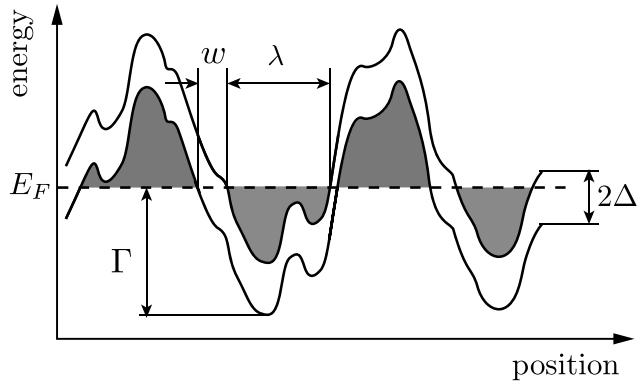

Fig. 2. Schematic picture of a cross section of puddles for the case of strong disorder, $\Gamma \gg \Delta$. The wavy lines show the conduction band bottom and the valence band ceiling separated by the gap 2Δ. The red shaded region above the Fermi level $E_F = 0$ represents a hole puddle, while the blue shaded region below E_F represents an electron puddle. Γ is the amplitude of the disorder potential, λ is the screening length, and w is the width of the barrier between neighboring puddles

than the energy gap that is expected theoretically or measured through local probes like optical absorption or scanning tunneling microscopy.

Here, we show that there is indeed no simple proportionality between the energy gap and the activation energy except at the highest temperature regime, which is likely irrelevant for many experimental contexts. Instead, we find a wide regime of temperature and disorder strength for which the activation energy is dramatically smaller than the energy gap. At the lowest temperatures the conductivity follows the Efros – Shklovskii (ES) law rather than an Arrhenius law, and this dependence can give the appearance of a small activation energy.

Let us dwell on two likely applications of our theory. First, our results may be especially relevant for ongoing efforts to understand the energy gaps arising in TBG at certain commensurate fillings of the moiré superlattice [27–31]. Such gaps apparently arise from electron–electron interactions, but the observed activation energies of the maximally insulating state are typically an order of magnitude smaller than the naive interaction scale (see, e.g., Refs. [28, 29]), and they vary significantly from one sample to another. Scanning tunneling microscopy studies also suggest a gap on the order of ten times larger than the observed activation energy [32, 33]. The theory we present here offers a natural way to interpret this discrepancy.

Second, our theory can be applied to the huge body of experimental work on thin films of 3D TI, where the surface electrons have a small gap 2Δ due to hybridiza-

tion of the surface states of two surfaces [8,9], or due to intentionally introduced magnetic impurities [10–24]. Understanding the origin of the small apparent activation energy $E_a \ll \Delta$ is crucial for achieving metrological precision of the quantum anomalous Hall effect [11,13,16,19–24,34–36] and the quantum spin Hall effect [9,37–39].

The model we consider is a two-dimensional semiconductor with band gap 2Δ atop a substrate with a three-dimensional concentration N of random sign charged impurities. We assume that the semiconductor has a gapped Dirac dispersion law

$$\epsilon^2(\mathbf{k}) = (\hbar v k)^2 + \Delta^2. \tag{1}$$

We are mostly interested in the case when the amplitude Γ of spatial fluctuations of the random potential satisfies $\Gamma \gg \Delta$, so that electron and hole puddles occupy almost half of the space each and are separated by a small insulating gap which occupies only a small fraction of the space (see Fig. 2). This system is an insulator because in 2D neither electron nor hole puddles percolate, and they are disconnected from each other. Throughout this paper we mostly focus on the case of zero chemical potential, for which electron and hole puddles are equally abundant and the system achieves its maximally insulating state. We argue that this situation is likely realized in the experiments of Refs. [5–33].

The remainder of this paper is organized as follows. In the following section we first summarize our main results for the temperature-dependent conductivity. Sections 3 and 4 concentrate on the case $\Gamma \gg \Delta$ illustrated by Fig. 2. In Sec. 3 we start from reviewing the fractal geometry of two-dimensional puddles and then calculate the action accumulated by electrons tunneling across the gap between two neighboring fractal metallic puddles, the corresponding localization length, and the critical value of the ratio Γ/Δ, at which crossover to weak localization takes place. In Sec. 4 we calculate the hopping conductivity for the case $\Gamma \gg \Delta$.

In Sec. 5 we study the illustrated by Fig. 1 case where the impurity concentration N is lower and present the parameters of NNH and VRH as functions of N. Section 6 studies what happens when the Fermi level moves away from the neutrality point. We arrive at the "phase diagram" of the re-entrant metal–insulator–metal (MIM) transition. Section 7 deals with the generalization of our results to thin TI films. Because of large interest to such films [8–10,12–24,34–49], in this section we add a fair amount of numerical estimates. In Sec. 8 we briefly return to the problem of three-dimensional, completely-compensated semiconductors with a gapped Dirac dispersion, and extend the previous theory [1–3] to the case when disorder potential fluctuations exceed Δ. We again arrive at a re-entrant MIM transition away from the neutrality point. We close in Sec. 9 with a summary and conclusion. Some results of this paper are published in its shorter version [50].

The results from the list of Refs. [1–85] are used or/and discussed in our work. The figures illustrating our results are presented below.

2. SUMMARY AND CONCLUSION

In this paper we have considered the temperature-dependent conductivity of a two-dimensional insulator subjected to disorder by Coulomb impurities in the substrate. Our primary results can be summarized as follows. When the impurity concentration N is below a certain value N_0 (see Eq. (6)), the random potential of charged impurities necessarily produces large band bending, which the amplitude Γ becomes much larger than Δ. Then the system can be described as a network of large and closely-spaced fractal puddles (Fig. 2) separated by narrow insulating barriers (Fig. 5). This disorder landscape implies low-energy pathways for electron conduction, leads to the "three-mechanism sequence" illustrated in Fig. 3. The high temperature regime with $E_a = \Delta$ is relegated to only such high temperatures that T is comparable to Δ. The second regime, the nearest neighbor hopping between puddles (NNH), exhibits a parametrically smaller activation energy, whose value depends on the impurity concentration. At the lowest temperatures the conductivity is due to the Efros–Shklovskii variable range hopping (VRH), which may appear as an even smaller activation energy when measured over a limited temperature range. Experiments are instead more likely to observe NNH or ES VRH, with an activation energy that declines very rapidly with increasing N (Fig. 4).

When the impurity concentration N exceeds another critical value N_c the tunnel barriers between puddles become thin enough to be nearly transparent, and electrons are delocalized across many puddles. In this limit the conductivity follows ES law with the localization length growing exponentially with increased disorder. The corresponding apparent activation energy falls exponentially, so that in mesoscopic samples one effectively has an unconventional disorder-induced insulator-to-metal transition (IMT). The analogous problem for three-dimensional insulators (see Sec. 8) shows

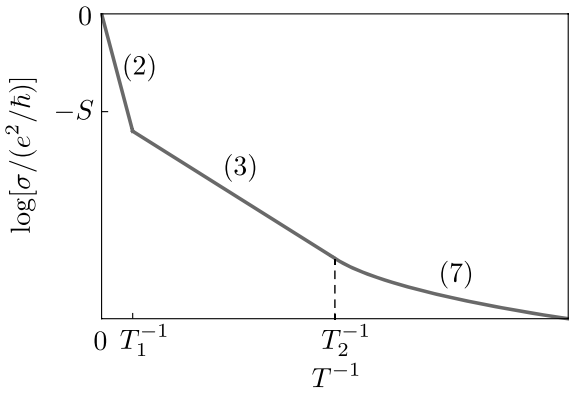

Fig. 3. Logarithm of the dimensionless conductivity $\sigma/(e^2/\hbar)$ as a function of the inverse temperature T^{-1} in the case $1 \ll \Gamma/\Delta \ll (\Gamma/\Delta)_c$. At high temperature $T > T_1$, the conductivity has activation energy Δ. At intermediate temperature $T_2 < T < T_1$, the conductivity is dominated by NNH. At low temperatures $T < T_2$, NNH is replaced by ES VRH. Numbers adjacent to different parts of the line show corresponding equations. Temperatures T_1 and T_2 are given by Eqs. (9) and (10)

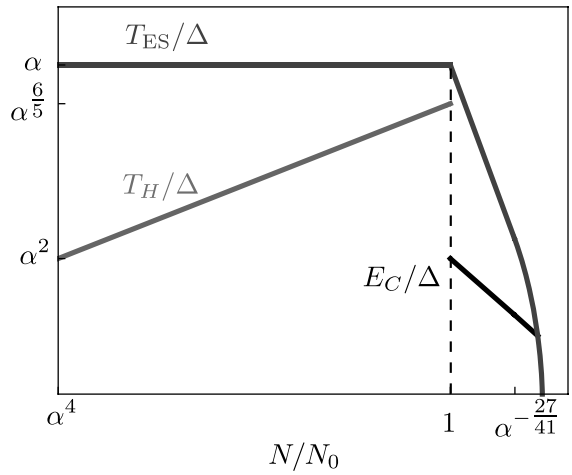

Fig. 4. Schematic log-log plots of characteristic energies of three kinds of hopping conductivity. The characteristic temperature of ES law T_{ES} (blue line), the activation energy of NNH, E_C (black solid line) and the characteristic temperature of hybrid conductivity T_H (red line) are shown as functions of the dimensionless impurity concentration $N/N_0 = (\Gamma/\Delta)^3$. The left part of the plot where $N/N_0 < 1$ corresponds to Eqs. (41) and (12), while the right part at $N/N_0 > 1$ corresponds to Eqs. (8) and (4). In the horizontal axis $N/N_0 = N_c/N_0 = \alpha^{-27/41}$ corresponds to $\Gamma/\Delta = (\Gamma/\Delta)_c$ given by Eq. (28). At this point $T_{ES} = \alpha^{87/41}\Delta$. When $\Gamma/\Delta > (\Gamma/\Delta)_c$ the localization length ξ increases exponentially and T_{ES} decreases exponentially

a genuine IMT due to percolation of electron and hole puddles separately.

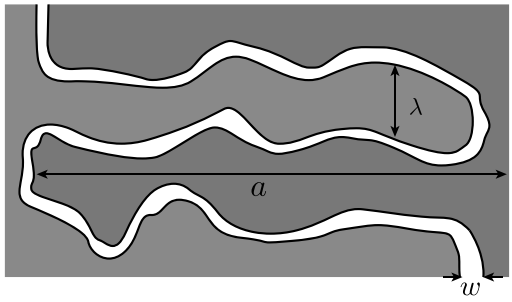

Fig. 5. Schematic picture of interlocked "fingers" of neighboring puddles. Here the length of "fingers" a is of order of the puddle diameter. One can imagine that Fig. 2 shows a vertical cross section of Fig. 5

Above we were talking about the neutrality point. When the Fermi level is away from neutrality point and the concentration of impurities is relatively small, there is a conventional metal–insulator transition with increasing disorder. Combining it with IMT at large impurity concentrations away from neutrality we arrive at a disorder driven re-entrant MIM transition. (See phase diagrams of such transitions shown in Fig. 7 and Fig. 9.)

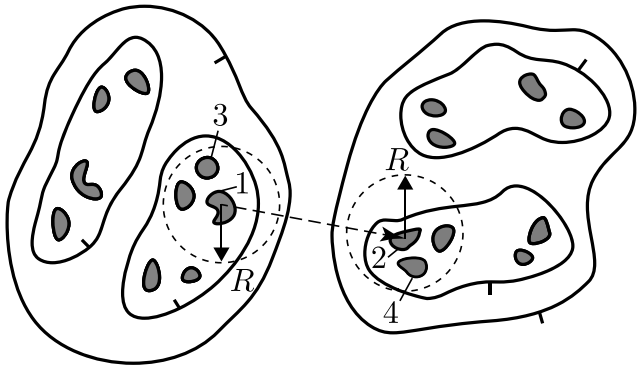

Fig. 6. Schematic map of nearest neighbor electron and hole puddles containing many electron (blue) and hole (red) puddles. The continuous lines are equipotential contours of the electron energy. As in geographical maps the direction of descent is indicated by a short stroke. The smallest contours represent boundaries of droplets at the chemical potential. The dashed arrow shows the shortest hop between the two puddles. At $T \ll T_1'$ electron searches in dashed circles of radius R for droplets 3 and 4 with closer to the chemical potential energies, which provide a smaller inter-puddle hop resistance

Our results have implications for a wide variety of experiments on 2D electron systems with a narrow energy gap. Some of these include 2D and thin 3D TIs, Bernal bilayer graphene with a perpendicular displacement field, and twisted bilayer graphene, as mentioned in the Introduction. In such systems the

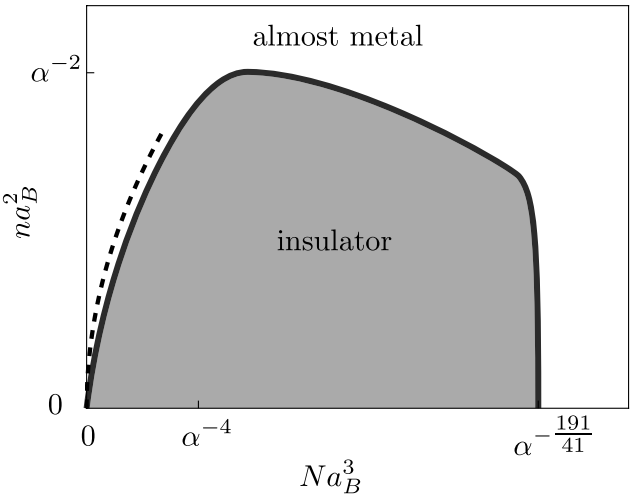

Fig. 7. Schematic n–N phase diagram in a two-dimensional semiconductor. The shaded blue domain is the insulator phase while the white domain is the almost metal phase. On the left (small N) side of the diagram the phase boundary follows Eq. (43) (dashed line) and reaches the maximum near $Na_B^3 = N_0 a_B^3 = \alpha^{-4}$. On the right side the maximum of the phase boundary is determined by criterion $G(n, N) = 1$ for tunneling between electron puddles. When with decreasing n this tunneling rate yields to the tunneling between electron and hole puddles, the boundary becomes vertical, i. e., sticks to the critical point $Na_B^3 = N_c a_B^3 = \alpha^{-191/41}$ all the way till $n = 0$ (cf. Eq. (28)). We use $\alpha = 0.12$ for this plot

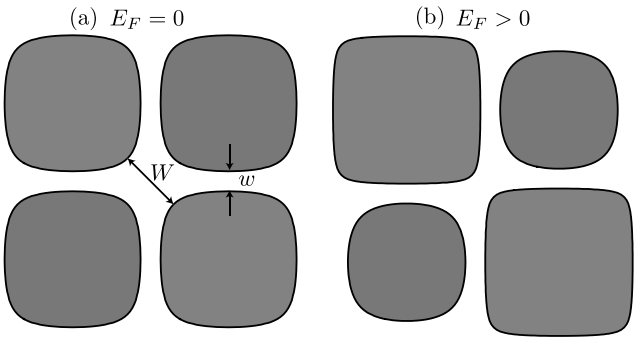

Fig. 8. Illustration of the competition of the two tunneling rates for a chessboard potential. Blue and red domains are the electron and hole puddles separated by insulating gap (white). *a*) At the neutrality point, $n = 0$, $E_F = 0$, the shortest tunneling distance between electron puddles W is much larger than the distance w between electron and hole puddles. *b*) At $E_F > 0$ and growing n, W decreases. Eventually it becomes smaller than w and vanishes at the percolation transition where all electron puddles merge into the infinite cluster

temperature-dependent conductivity is often used as a primary way to diagnose the magnitude of energy gaps. Our results here suggest that such studies suffer

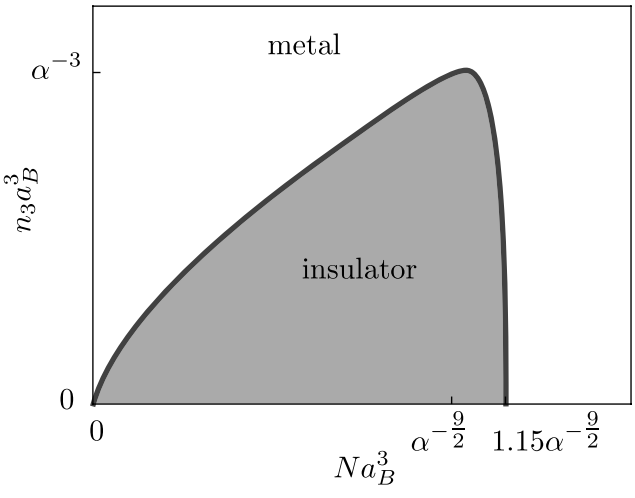

Fig. 9. Schematic n_3–N plane phase diagram of a 3D narrow gap strongly compensated semiconductor. The shaded blue domain is the insulator phase while the white domain is the metal phase. The phase boundary follows Eq. (65) on the left side, reaches the maximum $n_3 a_B^3 = \alpha^{-3}$ near $Na_B^3 = N_1 a_B^3 = \alpha^{-9/2}$, and then vertically drops at $N = N_c = 1.15 N_1$

an essentially unavoidable limitation, since the apparent activation energy E_a at low temperature has no simple relation to the energy gap, and in general E_a can be taken only as a weak lower bound. No wonder that the transport activation energy in many cases is 10–100 times smaller than the value expected theoretically or measured by probes like optical absorption or tunneling spectroscopy. In this paper we studied in details gapped thin films of 3D topological insulators, which due to the large dielectric constant have peculiar 3D-like electrostatics (see Sec. 7).

The existence of an apparent disorder-induced IMT in strongly compensated semiconductor is an especially striking result of our analysis. For conventional insulators, this apparent transition cannot be called a true IMT, since in 2D the zero-temperature conductance flows toward zero in the thermodynamic limit for any finite amount of disorder [83]. However, the situation may be different for thin TI films, since the spin-orbit coupling of the TI surface states permits a stable metallic phase [84, 85]. A full theory of this IMT in TI films is beyond the scope of our current analysis.

Finally, we mention that the tunneling between puddles can be reduced by applying a magnetic field orthogonal to the 2D plane. This reduction leads to an exponential positive magnetoresistance in the insulating phase, similar to the one studied in Ref. [2]. The theory of such magnetoresistance is also beyond the scope of this paper.

Acknowledgments. We are grateful to David Goldhaber-Gordon, Ilya Gruzberg, Shahal Ilani, Fai Mak, Koji Muraki, Stevan Nadj-Perge, and Christoph Stampfer for helpful discussions.

Funding. Y. H. is supported by the William I. Fine Theoretical Physics Institute. B. S. was partly supported by NSF grant DMR-2045742.

The full text of this paper is published in the English version of JETP.

REFERENCES

1. B. I. Shklovskii and A. L. Efros, Zh. Eksp. Theor. Fiz. **62**, 1156 (1972) [Sov. Phys. JETP **35**, 610 (1972)].

2. B. I. Shklovskii and A. L. Efros, *Electronic Properties of Doped Semiconductors*, Vol. 45, Springer, Berlin (1984).

3. B. Skinner, T. Chen, and B. I. Shklovskii, Phys. Rev. Lett. **109**, 176801 (2012).

4. T. Chen and B. Skinner, Phys. Rev. B **94**, 085146 (2016).

5. E. B. Olshanetsky, Z. D. Kvon, G. M. Gusev, A. D. Levin, O. E. Raichev, N. N. Mikhailov, and S. A. Dvoretsky, Phys. Rev. Lett. **114**, 126802 (2015).

6. Z. D. Kvon, D. A. Kozlov, E. B. Olshanetsky, G. M. Gusev, N. N. Mikhailov, and S. A. Dvoretsky, Phys. Usp. **63**, 629 (2020).

7. L. Pan, X. Liu, Q. L. He, A. Stern, G. Yin, X. Che, Q. Shao, P. Zhang, P. Deng, C.-Y. Yang, B. Casas, E. S. Choi, J. Xia, X. Kou, and K. L. Wang, Sci. Adv. **6**, eaaz3595 (2020).

8. D. Nandi, B. Skinner, G. H. Lee, K.-F. Huang, K. Shain, C.-Z. Chang, Y. Ou, S.-P. Lee, J. Ward, J. S. Moodera, P. Kim, B. I. Halperin, and A. Yacoby, Phys. Rev. B **98**, 214203 (2018).

9. S. K. Chong, L. Liu, K. Watanabe, T. Taniguchi, T. Sparks, F. Liu, and V. V. Deshpande, Nature Portfolio (2021), 10.21203/rs.3.rs-519444/v1.

10. J. G. Checkelsky, J. Ye, Y. Onose, Y. Iwasa, and Y. Tokura, Nature Phys. **8**, 729 (2012).

11. C.-Z. Chang, J. Zhang, X. Feng, J. Shen, Z. Zhang, M. Guo, K. Li, Y. Ou, P. Wei, L.-L. Wang, Z.-Q. Ji, Y. Feng, S. Ji, X. Chen, J. Jia, X. Dai, Z. Fang, S.-C. Zhang, K. He, Y. Wang, L. Lu, X.-C. Ma, and Q.-K. Xue, Science **340**, 167 (2013).

12. K. He, X.-C. Ma, X. Chen, L. Lu, Y.-Y. Wang, and Q.-K. Xue, Chinese Phys. B **22**, 067305 (2013).

13. M. Mogi, R. Yoshimi, A. Tsukazaki, K. Yasuda, Y. Kozuka, K. S. Takahashi, M. Kawasaki, and Y. Tokura, Appl. Phys. Lett. **107**, 182401 (2015).

14. L. Zhang, D. Zhao, Y. Zang, Y. Yuan, G. Jiang, M. Liao, D. Zhang, K. He, X. Ma, and Q. Xue, APL Materials **5**, 076106 (2017).

15. W. Wang, Y. Ou, C. Liu, Y. Wang, K. He, Q.-K. Xue, and W. Wu, Nature Phys. **14**, 791 (2018).

16. E. J. Fox, I. T. Rosen, Y. Yang, G. R. Jones, R. E. Elmquist, X. Kou, L. Pan, K. L. Wang, and D. Goldhaber-Gordon, Phys. Rev. B **98**, 075145 (2018).

17. J. Moon, J. Kim, N. Koirala, M. Salehi, D. Vanderbilt, and S. Oh, Nano Lett. **19**, 3409 (2019), pMID: 31038971.

18. I. T. Rosen, I. Yudhistira, G. Sharma, M. Salehi, M. A. Kastner, S. Oh, S. Adam, and D. Goldhaber-Gordon, Phys. Rev. B **99**, 201101 (2019).

19. Y. Okazaki, T. Oe, M. Kawamura, R. Yoshimi, S. Nakamura, S. Takada, M. Mogi, K. S. Takahashi, A. Tsukazaki, M. Kawasaki, Y. Tokura, and N.-H. Kaneko, Appl. Phys. Lett. **116**, 143101 (2020).

20. L. K. Rodenbach, I. T. Rosen, E. J. Fox, P. Zhang, L. Pan, K. L. Wang, M. A. Kastner, and D. Goldhaber-Gordon, APL Materials **9**, 081116 (2021).

21. K. M. Fijalkowski, N. Liu, P. Mandal, S. Schreyeck, K. Brunner, C. Gould, and L. W. Molenkamp, Nature Commun. **12**, 1 (2021).

22. G. M. Ferguson, R. Xiao, A. R. Richardella, D. Low, N. Samarth, and K. C. Nowack, arXiv:2112.13122 [cond-mat.mes-hall].

23. I. T. Rosen, M. P. Andersen, L. K. Rodenbach, L. Tai, P. Zhang, K. L. Wang, M. A. Kastner, and D. Goldhaber-Gordon, arXiv:2112.13123 [cond-mat.mes-hall].

24. Y. Okazaki, T. Oe, M. Kawamura, R. Yoshimi, S. Nakamura, S. Takada, M. Mogi, K. S. Takahashi, A. Tsukazaki, M. Kawasaki, Y. Tokura, and N.-H. Kaneko, Nature Phys. **18**, 25 (2022).

25. K. Zou and J. Zhu, Phys. Rev. B **82**, 081407 (2010).

26. T. Taychatanapat and P. Jarillo-Herrero, Phys. Rev. Lett. **105**, 166601 (2010).

27. M. Serlin, C. L. Tschirhart, H. Polshyn, Y. Zhang, J. Zhu, K. Watanabe, T. Taniguchi, L. Balents, and A. F. Young, Science **367**, 900 (2020).

28. P. Stepanov, I. Das, X. Lu, A. Fahimniya, K. Watanabe, T. Taniguchi, F. H. L. Koppens, J. Lischner, L. Levitov, and D. K. Efetov, Nature **583**, 375 (2020).

29. J. M. Park, Y. Cao, K. Watanabe, T. Taniguchi, and P. Jarillo-Herrero, Nature **592**, 43 (2021).

30. Y. Cao, V. Fatemi, A. Demir, S. Fang, S. L. Tomarken, J. Y. Luo, J. D. Sanchez-Yamagishi, K. Watanabe, T. Taniguchi, E. Kaxiras, R. C. Ashoori, and P. Jarillo-Herrero, Nature **556**, 80 (2018).

31. Y. Cao, V. Fatemi, S. Fang, K. Watanabe, T. Taniguchi, E. Kaxiras, and P. Jarillo-Herrero, Nature **556**, 43 (2018).

32. Y. Xie, B. Lian, B. Jäck, X. Liu, C.-L. Chiu, K. Watanabe, T. Taniguchi, B. A. Bernevig, and A. Yazdani, Nature **572**, 101 (2019).

33. Y. Choi, H. Kim, C. Lewandowski, Y. Peng, A. Thomson, R. Polski, Y. Zhang, K. Watanabe, T. Taniguchi, J. Alicea, and S. Nadj-Perge, Nature Phys. **17**, 1375 (2021).

34. R. Yu, W. Zhang, H.-J. Zhang, S.-C. Zhang, X. Dai, and Z. Fang, Science **329**, 61 (2010).

35. J. Zhang, C.-Z. Chang, P. Tang, Z. Zhang, X. Feng, K. Li, L. li Wang, X. Chen, C. Liu, W. Duan, K. He, Q.-K. Xue, X. Ma, and Y. Wang, Science **339**, 1582 (2013).

36. C.-Z. Chang, C.-X. Liu, and A. H. MacDonald, arXiv:2202.13902 [cond-mat.mes-hall].

37. C.-X. Liu, H. Zhang, B. Yan, X.-L. Qi, T. Frauenheim, X. Dai, Z. Fang, and S.-C. Zhang, Phys. Rev. B **81**, 041307(R) (2010).

38. H.-Z. Lu, W.-Y. Shan, W. Yao, Q. Niu, and S.-Q. Shen, Phys. Rev. B **81**, 115407 (2010).

39. J. Linder, T. Yokoyama, and A. Sudbø, Phys. Rev. B **80**, 205401 (2009).

40. Y. Zhang, K. He, C.-Z. Chang, C.-L. Song, L.-L. Wang, X. Chen, J.-F. Jia, Z. Fang, X. Dai, W.-Y. Shan, S.-Q. Shen, Q. Niu, X.-L. Qi, S.-C. Zhang, X.-C. Ma, and Q.-K. Xue, Nature Phys. **6**, 584 (2010).

41. Y. Sakamoto, T. Hirahara, H. Miyazaki, S.-i. Kimura, and S. Hasegawa, Phys. Rev. B **81**, 165432 (2010).

42. T. Zhang, J. Ha, N. Levy, Y. Kuk, and J. Stroscio, Phys. Rev. Lett. **111**, 056803 (2013).

43. D. Kim, P. Syers, N. P. Butch, J. Paglione, and M. S. Fuhrer, Nature Commun. **4**, 2040 (2013).

44. Y. L. Chen, J.-H. Chu, J. G. Analytis, Z. K. Liu, K. Igarashi, H.-H. Kuo, X. L. Qi, S. K. Mo, R. G. Moore, D. H. Lu, M. Hashimoto, T. Sasagawa, S. C. Zhang, I. R. Fisher, Z. Hussain, and Z. X. Shen, Science **329**, 659 (2010).

45. S.-Y. Xu, M. Neupane, C. Liu, D. Zhang, A. Richardella, L. Andrew Wray, N. Alidoust, M. Leandersson, T. Balasubramanian, J. Sánchez-Barriga, O. Rader, G. Landolt, B. Slomski, J. Hugo Dil, J. Osterwalder, T.-R. Chang, H.-T. Jeng, H. Lin, A. Bansil, N. Samarth, and M. Zahid Hasan, Nature Phys. **8**, 616 (2012).

46. M. Ye, W. Li, S. Zhu, Y. Takeda, Y. Saitoh, J. Wang, H. Pan, M. Nurmamat, K. Sumida, F. Ji, Z. Liu, H. Yang, Z. Liu, D. Shen, A. Kimura, S. Qiao, and X. Xie, Nature Commun. **6**, 8913 (2015).

47. Y. Tokura, K. Yasuda, and A. Tsukazaki, Nature Rev. Phys. **1**, 126 (2019).

48. Y. Deng, Y. Yu, M. Z. Shi, Z. Guo, Z. Xu, J. Wang, X. H. Chen, and Y. Zhang, Science **367**, 895 (2020).

49. R. Lu, H. Sun, S. Kumar, Y. Wang, M. Gu, M. Zeng, Y.-J. Hao, J. Li, J. Shao, X.-M. Ma, Z. Hao, K. Zhang, W. Mansuer, J. Mei, Y. Zhao, C. Liu, K. Deng, W. Huang, B. Shen, K. Shimada, E. F. Schwier, C. Liu, Q. Liu, and C. Chen, Phys. Rev. X **11**, 011039 (2021).

50. Y. Huang, Y. He, B. Skinner, and B. I. Shklovskii, Phys. Rev. B **105**, 054206 (2022).

51. T. Chen, B. Skinner, and B. I. Shklovskii, Phys. Rev. Lett. **109**, 126805 (2012).

52. J. Zhang and B. I. Shklovskii, Phys. Rev. B **70**, 115317 (2004).

53. E. McCann and M. Koshino, Rep. Prog. Phys. **76**, 056503 (2013).

54. S. Slizovskiy, A. Garcia-Ruiz, A. I. Berdyugin, N. Xin, T. Taniguchi, K. Watanabe, A. K. Geim, N. D. Drummond, and V. I. Fal'ko, Nano Lett. **21**, 6678 (2021), pMID: 34296602.

55. M. B. Isichenko, Rev. Mod. Phys. **64**, 961 (1992).

56. B. Skinner and B. I. Shklovskii, Phys. Rev. B **87**, 075454 (2013).

57. B. I. Shklovskii and A. L. Efros, Zh. Eksp. Theor. Fiz. **59**, 1343 (1970) [Sov. Phys. JETP **32**, 733 (1971)].

58. M. E. Raikh and I. M. Ruzin, Sov. Phys. Semicond. **19**, 745 (1985).

59. H. Samavati, A. Hajimiri, A. Shahani, G. Nasserbakht, and T. Lee, IEEE J. Solid-State Circuits **33**, 2035 (1998).

60. A. L. Efros and B. I. Shklovskii, J. Phys. C: Sol. St. Phys. **8**, L49 (1975).

61. B. I. Shklovskii, Low Temp. Phys. **43**, 699 (2017) [Fizika Nizkikh Temperatur **43**, 879 (2017)].

62. B. I. Shklovskii, Fizika i Tekhnika Poluprovodnikov **7**, 112 (1973) [Sov. Phys. Semicond. **7**, 77 (1973)].

63. Y. Huang, Y. Ayino, and B. I. Shklovskii, Phys. Rev. Mater. **5**, 044606 (2021).

64. T. Li, S. Jiang, L. Li, Y. Zhang, K. Kang, J. Zhu, K. Watanabe, T. Taniguchi, D. Chowdhury, L. Fu, J. Shan, and K. F. Mak, Nature **597**, 350 (2021).

65. A. Ghiotto, E.-M. Shih, G. S. S. G. Pereira, D. A. Rhodes, B. Kim, J. Zang, A. J. Millis, K. Watanabe, T. Taniguchi, J. C. Hone, L. Wang, C. R. Dean, and A. N. Pasupathy, Nature **597**, 345 (2021).

66. W. Richter and C. R. Becker, Phys. Stat. Sol. (b) **84**, 619 (1977).

67. N. Borgwardt, J. Lux, I. Vergara, Z. Wang, A. A. Taskin, K. Segawa, P. H. M. van Loosdrecht, Y. Ando, A. Rosch, and M. Grüninger, Phys. Rev. B **93**, 245149 (2016).

68. T. Bömerich, J. Lux, Q. T. Feng, and A. Rosch, Phys. Rev. B **96**, 075204 (2017).

69. J. Zhang, C.-Z. Chang, Z. Zhang, J. Wen, X. Feng, K. Li, M. Liu, K. He, L. Wang, X. Chen, Q.-K. Xue, X. Ma, and Y. Wang, Nature Commun. **2**, 574 (2011).

70. N. S. Rytova, Moscow Univ. Phys. Bull. **3**, 18 (1967).

71. A. Chaplik and M. Entin, JETP **34**, 1335 (1971) [Zh. Eksp. Teor. Fiz. **61**, 2496 (1971)].

72. L. V. Keldysh, JETP Lett. **29**, 658 (1979) [Pis'ma v Zh. Eksp. Teor. Fiz. **29**, 716 (1979)].

73. Y. Huang and B. I. Shklovskii, Phys. Rev. B **103**, 165409 (2021).

74. Y. Huang and B. I. Shklovskii, Phys. Rev. B **104**, 054205 (2021).

75. H. Weng, X. Dai, and Z. Fang, Phys. Rev. X **4**, 011002 (2014).

76. M. K. Tran, J. Levallois, P. Lerch, J. Teyssier, A. B. Kuzmenko, G. Autès, O. V. Yazyev, A. Ubaldini, E. Giannini, D. van der Marel, and A. Akrap, Phys. Rev. Lett. **112**, 047402 (2014).

77. A. Ohmura, Y. Higuchi, T. Ochiai, M. Kanou, F. Ishikawa, S. Nakano, A. Nakayama, Y. Yamada, and T. Sasagawa, Phys. Rev. B **95**, 125203 (2017).

78. S. Singh, A. C. Garcia-Castro, I. Valencia-Jaime, F. Mu noz, and A. H. Romero, Phys. Rev. B **94**, 161116 (2016)

79. D. Vu, W. Zhang, C. Şahin, M. E. Flatté, N. Trivedi, and J. P. Heremans, Nature Mater. **20**, 1525 (2021).

80. B. Skinner, Phys. Rev. B **90**, 060202 (2014).

81. D. G. Polyakov and B. I. Shklovskii, Phys. Rev. B **48**, 11167 (1993).

82. B. I. Shklovskii and A. L. Efros, Zh. Eksp. Theor. Fiz. **60**, 867 (1971) [Sov. Phys. JETP **33**, 468 (1971)].

83. E. Abrahams, P. W. Anderson, D. C. Licciardello, and T. V. Ramakrishnan, Phys. Rev. Lett. **42**, 673 (1979).

84. S. Hikami, A. I. Larkin, and Y. Nagaoka, Progr. Theor. Phys. **63**, 707 (1980).

85. R. S. K. Mong, J. H. Bardarson, and J. E. Moore, Phys. Rev. Lett. **108**, 076804 (2012).